Environmental Research Communications

PAPER

Present and future diurnal hourly precipitation in 0.11° EURO-CORDEX models and at convection-permitting resolution

Edmund P Meredith[1], **Uwe Ulbrich**[1], **Henning W Rust**[1] **and Heimo Truhetz**[2]

[1] Institut für Meteorologie, Freie Universität Berlin, Carl-Heinrich-Becker-Weg 6-10, 12165 Berlin, Germany
[2] Wegener Center for Climate and Global Change, University of Graz, Graz, Austria

E-mail: edmund.meredith@met.fu-berlin.de

Keywords: diurnal cycle, hourly precipitation, extreme precipitation, CORDEX, convection-permitting model, climate change

Supplementary material for this article is available online

OPEN ACCESS

RECEIVED
23 October 2020

REVISED
22 March 2021

ACCEPTED FOR PUBLICATION
24 March 2021

PUBLISHED
21 May 2021

Abstract

The diurnal cycle of precipitation (DCP) is a core mode of precipitation variability in regions and seasons where the dominant precipitation type is convective. The occurrence of extreme precipitation is often closely linked to the DCP. Future changes in extreme precipitation may furthermore, in certain regions, exhibit a strong diurnal signal. Here we investigate the present and future diurnal cycle of hourly precipitation in the state-of-the-art 0.11°C EURO-CORDEX (EC-11) ensemble and in a convection-permitting model (CPM), with a focus on extremes. For the present climate, long-standing timing and frequency biases in the DCP found in lower-resolution models persist in the EC-11 ensemble. In the CPM, however, these biases are largely absent, particularly the diurnal distribution of extremes, which the EC-11 ensemble misrepresents. For future changes to hourly precipitation, we find clear diurnal signals in the CPM and in EC-11 models, with high regional and intra-ensemble variability. The diurnal signal typically peaks in the morning. Interestingly, the EC-11 ensemble mean shows reasonable agreement with the CPM on the diurnal signal's timing, showing that this feature is representable by models with parametrized convection. Comparison with the CPM suggests that EC-11 models greatly underestimate the amplitude of this diurnal signal. Our study highlights the advantages of CPMs for investigating future precipitation change at the diurnal scale, while also showing the EC-11 ensemble capable of detecting a diurnal signal in future precipitation change.

1. Introduction

Precipitation is one of numerous meteorological variables which exhibit diurnal cycles, all stemming directly or indirectly from accumulated surface heating via the diurnal cycle of solar insolation. Other examples include temperature, cloudiness, relative humidity and local winds [1–8]. For precipitation, the mean diurnal cycle is most pronounced in non-arid regions where the dominant precipitation type is convective: the tropical rain belts, along with parts of the subtropics and extratropics during summer [9, 10]. Observational studies show that the mean diurnal cycle of precipitation (DCP) reaches its maximum during the late afternoon to early evening [7, 11–15], as accumulated surface heating brings boundary layer temperatures towards the convective temperature, thus allowing built-up convective available potential energy (CAPE) to be consumed by convection. Exceptions to the DCP late-afternoon to early-evening peak can be found over tropical oceans [8, 16], where a nocturnal maximum exists, as well as in regions where mesoscale convective systems form during the afternoon before associated squall lines propagate into neighbouring areas over timescales of hours to days, and in regions where moisture convergence due to nocturnal low level jets causes precipitation [13, 17, 18]. The diurnal cycle is also evident in the diurnal timing of intense to extreme precipitation events [4, 14, 19, 20]. The DCP exerts strong influence on other variables, impacting temperature, humidity and more.

The central importance of the DCP to the Earth system has lead to its use as a key metric for evaluation of precipitation in climate models, in terms of intensity, frequency and the amplitudes of the respective cycles.

Traditionally, both general circulation models (GCMs) and even higher-resolution regional climate models (RCMs) have tended to inadequately recreate the DCP, raising questions about their utility for projecting future changes in the DCP. The most prominent errors in the simulated DCP are a premature peak in the diurnal maximum intensity and frequency, and an excessive amplitude [13, 15, 21–26]. This results from convection being triggered too often and too early in lower-resolution models, with CAPE not accumulating long enough for intense convective episodes to be realized. These shortcomings appear to be primarily a problem of convection parametrization schemes rather than simply too-low model resolution [23, 27]: models whose spatial resolution is too coarse to explicitly resolve deep convective processes must instead employ parametrization schemes to estimate the bulk effects of unresolved deep convection over each grid cell, redistributing heat and moisture in the atmospheric column accordingly and producing precipitation as a by-product [28, 29].

Despite their imperfect representation of the DCP, high-resolution RCMs still add considerable value to GCMs for multiple variables [30–34], producing valuable high-resolution climate data for end users. This added value serves as the motivation for the coordinated downscaling experiment CORDEX [35] and has its origins in the better representation of surface forcings (topography, land-sea contrasts, etc.) and mesoscale dynamics at higher resolution, which can more realistically interact with the large scales. Added value is thus most evident in regions where surface forcings show strong fine-scale variability and for variables such as precipitation which vary strongly at small scales [31, 36, 37]. In particular for precipitation, RCMs add the most value at the tail of the distribution, as precipitation extremes tend to be highly variable in space [36]. Added value is, of course, dependent on the GCM providing realistic large-scale boundary conditions; RCMs can not, in general, correct large-scale circulation errors present in their parent GCMs [34] and may even produce unrealistic secondary circulations [38–40]. To reduce remaining precipitation biases in RCMs—premature convective triggering and precipitation extremes which are too temporally persistent and too spatially diffuse [41, 42]—convection-permitting resolution ($\triangle x \leqslant 4$ km) must be achieved. Convection-permitting models (CPMs) can explicitly resolve deep convection, thus eliminating the need for its parametrization, and both improve the timing of the DCP and simulate more realistic subdaily precipitation extremes [24, 41–50] more realistic convective cloud cover [3] is also found. New research shows that the high-quality representation of precipitation in CPMs can also be found at subhourly timescales from both Eulerian [51] and Lagrangian [52, 53] perspectives.

Importantly, the added value of CPMs may also extend to the representation of the climate change signal [54, 55]. Standard thermodynamical arguments suggest that extreme precipitation events should intensify by roughly 6.5% per degree of warming [56–58] ('scaling') following the Clausius-Clapeyron (CC) relation, which relates the saturation vapour pressure of water to temperature. Some CPM studies show the potential for subdaily extreme precipitation to exhibit an amplified scaling in response to enhanced boundary forcing compared to lower-resolution RCMs with parametrized convection [55], potentially exceeding the CC scaling rate [45, 54].

Recently, *Meredith, Ulbrich and Rust* (2019)—henceforth MUR19—showed with a CPM for a region of western Europe that the scaling of extreme summertime (JJA) precipitation in response to climate change may itself exhibit a strong diurnal signal, with an AM maximum and a PM minimum. While diurnal differences in historical and future near-surface warming are a robust signal found globally over multiple regions in observations and many climate models [59–61], whether the diurnal differences in the future scaling of extreme precipitation found in MUR19 are a common feature across multiple regions and models remains unclear. Diurnal differences in future changes to other characteristics of the DCP (e.g. all-hour intensity, wet-hour intensity and frequency) have also not been compared across multiple regions and models, in particular at hourly resolution or in the state-of-the-art 0.11° EURO-CORDEX (EC-11) ensemble [62, 63].

The present study thus uses the EC-11 ensemble and the CPM used by MUR19 at hourly resolution to address the following questions. (1) Does the EC-11 ensemble also exhibit a diurnal signal for future precipitation changes? (2) If so, how does this differ from that found in the CPM (forced by one of the EC-11 RCMs) with respect to the amplitude of the signal and the time-of-day of its minimum and maximum? (3) Are there systematic differences in the diurnal signal across regions and models? (4) Can these systematic differences be linked to diurnal changes in other meteorological parameters? These investigations of the climate change signal are preceded by an observations-based evaluation of the present-climate hourly DCP in a CPM and the EC-11 ensemble, in particular to assess whether timing biases in the DCP maximum are dependent on event intensity. Any detected biases are used as guidance in interpreting the plausibility of the predicted diurnal signals of future precipitation change. Differences and/or similarities between the diurnal signals of future precipitation change in the CPM and EC-11 ensemble are furthermore used to draw inferences as to the underlying drivers of the diurnal signal.

2. Data and methods

2.1. EURO-CORDEX 0.11° regional climate model ensemble

EURO-CORDEX is an international dynamical downscaling collaboration using RCMs to produce a high-resolution multi-model ensemble of climate data for Europe [62, 63]. We use the highest available spatial resolution (0.11°) from this initiative. EC-11 RCMs forced by reanalysis well recreate the core features of European mean climatology, though with remaining biases in precipitation and temperature [64]. EC-11 RCMs have additionally been shown to add value to their 0.44° resolution counterparts for the representation of both mean and extreme precipitation at daily and 3-hourly timescale, primarily due to a better representation of orography and mesoscale convective dynamics [37, 65]. The first study of hourly summertime precipitation in a subset of EC-11 RCMs [66] found a remaining general underestimation of extreme intensities and a poor representation of their spatial patterns at the hourly timescale, in line with other RCM studies at comparable resolution [42]. The individual RCMs in the EC-11 ensemble were additionally found to be the dominant factor in determining the spatial structure of short-duration precipitation extremes, compared to the influence of their parent GCMs. Whether the added value of RCMs for extreme precipitation (see Introduction) extends to their related climate change signals is still a topic of research [32], with some examples having been demonstrated [37]. What is clear, is that there can be considerable spread in the precipitation projections of different RCMs, even when forced by the same GCM [32, 67, 68]. This uncertainty is highest for local-scale processes such as summertime convection and necessitates the use of large GCM-RCM ensembles to fully characterize the uncertainty in precipitation projections and reliably detect any anthropogenically-forced regional signals [32, 69].

We thus create a multi-model ensemble based on 12 different EC-11 GCM-RCM combinations and 4 different reanalysis-forced EC-11 RCMs for which we could obtain hourly precipitation data (table 1). We use this ensemble as the basis for both observations-based evaluation and future projections. Part of this multi-model ensemble is based on RCMs forced by free-running GCMs, meaning that RCMs could inherit biases from their parent GCMs, unlike those RCMs forced by reanalysis. Detected biases in these cases are thus reflective of the GCM-RCM combination rather than just the RCM. Evidence suggests, however, that biases across the modelling chain are not necessarily additive and that RCMs can reduce the biases found in GCMs [70].

For evaluation, we consider the period 2001-2018 based on the temporal coverage of our observational dataset (section 2.3). For the GCM-forced RCMs, the years 2001–2005 are based on historical CO_2 concentrations and the years 2006-2018 on the RCP8.5 scenario. The actual choice of RCP scenario here is of little significance, as between the different RCP scenarios there is minimal divergence in CO_2 concentrations prior to 2020. The years 2001-2018 in the GCM-RCM combinations don't correspond to the observed years 2001-2018 in terms of individual observed events, but as we're comparing multi-year climatologies over large scales this is of little relevance. As part of the evaluation experiment, we additionally make use of ERA-Interim reanalysis [71] driven EC-11 simulations. Due to limited data availability, only four reanalysis-forced RCMs are used and of these only two extend to 2018, with the other two covering only as far as 2010 and 2012 (table 1). The ERA-Interim forced simulations help in assessing the impact of the free-running GCMs on any detected biases in the EC-11 RCMs' diurnal cycles. Years 2001-2008 of the reanalysis-forced COSMO-CLM (CCLM, [72] runs were simulated by the CLM-Community (https://www.clm-community.eu/) as part of EURO-CORDEX, with years 2009-2018 simulated by the present authors using identical model version and configuration [73, 74].

For our climate change analyses, future projections are based on 2070-2099 under the RCP8.5 scenario, while the years 1970–1999 represent the historical climate. All 0.11° CCLM simulations (evaluation and climate change) used model version 4.8_clm17; we refer to this setup as CCLM-11.

2.2. Convection-permitting simulations

We perform a single convection-permitting simulation with the CCLM for both the evaluation (2001–2018) and climate change (1970–1999, 2070–2099) experiments (table 1). CCLM is the community model of the German regional climate research community, jointly further developed by the CLM-Community. For the evaluation experiment, CCLM version 5.0_clm16 is run at 0.025° resolution (CCLM-025) over a domain centred on Germany (figure 1). Initial and lateral boundary conditions come from the ERA-Interim driven CCLM-11 simulations described in section 2.1. For the climate change experiment, CCLM version 4.8_clm17 is run at 0.02° resolution (CCLM-02) over the MUR19 domain, covering western Germany, the Benelux countries and parts of France (figure 1). Lateral and initial boundary conditions come from the CCLM-11 EURO-CORDEX runs forced by the MPI-ESM-LR model [75], i.e. the member used in our EC-11 ensemble (table 1). The CCLM-02 simulations are described in detail in MUR19 and [74]. The CCLM-02 and CCLM-025 simulations are both time-slices from April to August each year, with April and May discarded for soil moisture spinup. In both CPM

Table 1. Model simulations. (**1-12**) GCM-RCM combinations from the 0.11° EURO-CORDEX ensemble used in the analysis. The experiment code is based on the CMIP5 protocol, where **r** denotes the realization, **i** the initialization method, and **p** the model physics of the GCM. The convective parametrization scheme refers to that of the RCM. (**i-iv**) ERA-Interim reanalysis forced EC-11 combinations used in the evaluation experiment (Section 3.1); note that two of these combinations cover less than the full 2001-2018 observations period. (**a-b**) The two convection-permitting simulations used in this study.

	Name	RCM	Convection scheme	GCM	Experiment	Institute
1	CNRM-CM5-ALADIN63	ALADIN63	PCMT [102, 103]	CNRM-CM5	r1i1p1	CNRM
2	HadGEM2-ES-ALADIN63	ALADIN63	—"—	MOHC-HadGEM2-ES	r1i1p1	CNRM
3	CNRM-CM5-CCLM4-8-17	CCLM4-8-17	Tiedtke [29]	CNRM-CM5	r1i1p1	CLMcom
4	EC-EARTH-CCLM4-8-17	CCLM4-8-17	—"—	ICHEC-EC-EARTH	r12i1p1	CLMcom
5	MPI-ESM-LR-CCLM4-8-17	CCLM4-8-17	—"—	MPI-ESM-LR	r1i1p1	CLMcom
6	HadGEM2-ES-HadREM3-GA7-05	HadREM3-GA7-05	Gregory & Rowntree [104]	MOHC-HadGEM2-ES	r1i1p1	MOHC
7	EC-EARTH-HadREM3-GA7-05	HadREM3-GA7-05	—"—	ICHEC-EC-EARTH	r12i1p1	MOHC
8	IPSL-CM5A-MR-RCA4	RCA4	Kain-Fritsch [105, 106]	IPSL-CM5A-MR	r1i1p1	SMHI
9	HadGEM2-ES-RCA4	RCA4	—"—	MOHC-HadGEM2-ES	r1i1p1	SMHI
10	MPI-ESM-LR-RCA4	RCA4	—"—	MPI-ESM-LR	r3i1p1	SMHI
11	MPI-ESM-LR-RegCM4-6	RegCM4-6	Tiedkte [29]	MPI-ESM-LR	r1i1p1	ICTP
12	MPI-ESM-LR-REMO2015	REMO2015	Tiedtke, Nordeng [29, 107]	MPI-ESM-LR	r3i1p1	GERICS

	Name	RCM	Convection scheme	Reanalysis	Years	Insitute (s)
i	ERAINT-CCLM4-8-17	CCLM4-8-17	Tiedtke [29]	ERA-Interim	2001-2018	FU Berlin CLMcom
ii	ERAINT-RCA4	RCA4	Kain-Fritsch [105, 106]	ERA-Interim	2001-2010	SMHI
iii	ERAINT-ALADIN63	ALADIN63	PCMT [102, 103]	ERA-Interim	2001-2018	CNRM
iv	ERAINT-HadREM3-GA07-05	HadREM3-GA07-05	Gregory & Rowntree [104]	ERA-Interim	2001-2012	MOHC

	Name	RCM	Convection scheme	Parent	Expt./Years	Insitute
a	CCLM-02 ($\triangle x = 0.02°$)	CCLM4-8-17	None	5 (above)	r1i1p1	FU Berlin
b	CCLM-025 ($\triangle x = 0.025°$)	CCLM5-0-16	None	i (above)	2001-2018	FU Berlin

simulations, deep convection is explicitly represented and shallow convection is parametrized based on a modified Tiedtke scheme [29].

2.3. Observations

Evaluation is based on the RADKLIM dataset [76]. RADKLIM is a gridded precipitation climatology for Germany derived from radar-based precipitation estimates at 5-minute frequency. Hourly sums are then derived and adjusted with gauge-based precipitation measurements. The spatial resolution is 1 km.

2.4. Analysis of present and future diurnal hourly precipitation

As our focus is on characteristics of the diurnal precipitation cycle, all analyses are concentrated on the summer months (JJA), where the diurnal cycle in Europe is most pronounced. Prior to analysis, all higher resolution data (observations, CPMs) are spatially aggregated to the CCLM-11 grid. For the evaluation experiment (section 3.1), we first compare the representation of the all-hour mean precipitation, wet-hour mean precipitation and wet-hour frequency for each hour-of-day in the 0.11° RCMs and CCLM-025 against observations. Wet-hours are defined as hours with $P \geqslant 0.1$ mm; increasing the wet-hour threshold to account for lighter precipitation events potentially being under-captured in the observational radar climatology does not affect the conclusions. This is

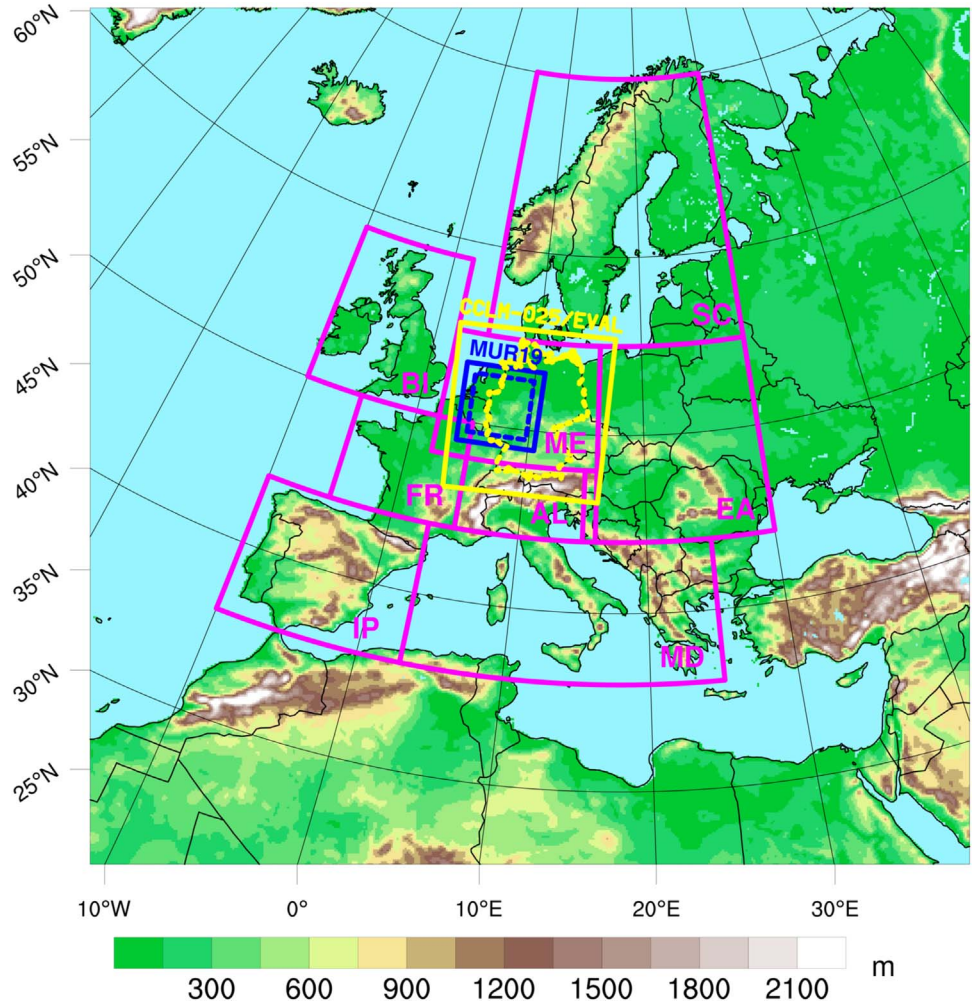

Figure 1. Simulation domains and analysis regions. The EURO-CORDEX simulation domain; shading shows orography as represented in the 0.11° CCLM. The 8 PRUDENCE regions are marked in magenta; the full names of each PRUDENCE region can be seen in figures 4-6. The MUR19 CCLM-02 simulation domain (solid) and analysis region (dashed) are marked in blue. The CCLM-025 simulation domain (solid) and analysis region (dashed) are marked in yellow.

followed by an assessment of the diurnal distribution of intense to extreme hourly precipitation events. Here, intense to extreme quantiles of hourly precipitation are computed from the whole analysis period, i.e. without hour-of-day partitioning, and the relative probabilities that these quantiles will be exceeded at a given hour-of-day are computed. The relative probabilities are with respect to the least probable hour, so that the least probable hour for threshold exceedance has a relative probability of 1. Evaluation is restricted to Germany, based on the spatial extent of RADKLIM.

For the climate change experiment, we assess diurnal differences in future changes to the character of hourly precipitation, with a focus on the scaling (%/K) of intense to extreme precipitation across the diurnal cycle and how this compares to the theoretical CC scaling rate (section 3.2), following MUR19. "Scaling"—sometimes referred to as "trend scaling" [77]—is the percentage change in extreme precipitation intensity per degree of climate warming; we use the 2 m temperature to represent warming. These analyses are performed with the EC-11 data on a regional basis by using the different European regions proposed in the PRUDENCE project [78]; the PRUDENCE region 'Mid Europe' corresponds closely to Germany (figure 1), used in the observations-based evaluation. We additionally compare the EC-11 results with those from the convection-permitting CCLM-02 runs over the MUR19 analysis region (figure 1). All diurnal curves are plotted on a common time axis, namely Central European Summer Time (CEST, UTC+2). We complete our analyses by assessing variables whose future changes may be related to whether or not a region or model exhibits a prominent diurnal signal for the future scaling of precipitation extremes (section 3.3). Here, each 24-hour diurnal scaling curve (region, GCM-RCM) is split into two 12-hour periods—the 'AM' and 'PM' periods (0100-1200, 1300-0000 CEST)—and the period and hour with minimum scaling is identified. The hour from the remaining period in which scaling is a maximum is then determined. This gives a peak-to-trough amplitude for each diurnal scaling curve (region, GCM-RCM) and the corresponding hours-of-day for which linear regression models based on differences in

other variables can be considered. This analysis is hampered by the limited availability of diagnostic variables at subdaily resolution for the EC-11 ensemble, meaning that not all mechanisms identified in MUR19 can be tested. Apart from precipitation, the highest available temporal resolution is 3-hourly. For consistency, CCLM-02 data are also considered at 3-hourly resolution where this is the available temporal resolution for the EC-11 data (i.e. non-precipitation data). To get to hourly resolution, a 6th-order polynomial function is thus fitted to the 3-hourly diurnal cycles of other variables where necessary (figure S 1). The statistical significance of the associations between the amplitude of the diurnal scaling signal and the other considered variables is assessed with the non-parametric Kendall's tau statistic, based on a two-tailed test and a null hypothesis that the variables have no association.

It is finally worth noting that some of the areas within the PRUDENCE regions, i.e. those with a Mediterranean climate, often experience their most intense convective events in the autumn [51, 79, 80]. These events are however typically associated with transiting cyclonic systems and are thus subject to minimal diurnal variability.

3. Results and discussion

3.1. Representation of the diurnal cycle of hourly precipitation for the present climate

A standard diagnostic for defining the DCP is the mean all-hour precipitation at each hour of the day [13, 21, 24, 15], giving a DCP which is a function of both wet-hour intensity and frequency. Models' diurnal biases in these two parameters may differ. Model biases in the DCP could also vary depending on event intensity. In this section we evaluate whether biases in the modelled all-hour DCP, including timing biases, differ from the diurnal biases found for precipitation frequency and higher precipitation intensities in (i) EC-11 RCMs forced with free-running GCMs, (ii) EC-11 RCMs forced with reanalysis and (iii) the CCLM-025 CPM nested in the reanalysis-forced CCLM-11. The analysis region is Germany, the period 2001-2018 and the season JJA.

EC-11 RCMs produce an unambiguous diurnal cycle for the all-hour mean DCP. The daily maximum occurs 3-4 hours earlier (ensemble mean; figure 2(a)) than the 1800-1900 CEST observed diurnal hourly maximum (figure 2(b)), however, suggesting premature convective triggering. Despite the temporal shift, the EC-11 ensemble mean diurnal cycle displays an appropriate amplitude and reasonable precipitation magnitudes outside of the peak hours. The former potentially represents an improvement on the excessive amplitudes found in lower-resolution models [21, 26]. The timing of the cycle matches the classic DCP known for models with parametrized convection and documented elsewhere [21, 15, 41, 42]. Interestingly, there is an ensemble spread of 3 hours in the timing of the diurnal maximum. For a given RCM, however, using reanalysis (figure 2(b)) or different GCMs as boundary forcing has no influence on the timing of the diurnal maximum (CCLM4-8-17, RCA4, ALADIN63, HadREM-GA7-05). The best performing EC-11 ensemble members come closer to the timing of the observed peak, with diurnal maxima just two hours earlier than in observations, while the worst-performing members have their maxima up to five hours too early. No EC-11 RCM has a delayed diurnal maximum. The fact that reanalysis-forced RCMs exhibit the same premature onset of convection as when forced with free-running GCMs (Figure 2(b)) indicates that this is a general problem of models reliant on convective parametrizations: at convection-permitting resolution, CCLM-025 produces an all-hour mean DCP which both peaks at the same time as in observations, correcting the 5-hour-early maximum found in its parent reanalysis-forced CCLM-11, and shows hourly magnitudes close to those observed (figure 2(b)).

To gain insight into the modelled biases in the all-hour mean DCP, we consider the associated underlying event intensities (i.e. wet-hour means) and frequencies (figures 2(c)–(f)). Here, stronger disagreement emerges between EC-11 RCMs and observations, and within the EC-11 ensemble itself. Across the diurnal cycle, EC-11 RCMs exhibit wet-hour means which are insufficiently intense. Many EC-11 RCMs (esp. CCLM, RegCM) furthermore exhibit a late-afternoon *minimum* in their wet-hour mean diurnal cycle, where observations approach their maximum. Only two EC-11 RCMs (RCA4, REMO2015) show wet-hour diurnal maxima whose timings match their all-hour equivalents, otherwise the wet-hour mean diurnal maxima occur during the night, in contrast to the mid-afternoon all-hour mean diurnal maxima. For the diurnal cycle of wet-hour frequency, the EC-11 ensemble exhibits closer intra-ensemble agreement and a timing bias like that of the all-hour mean: a diurnal maximum 3-4 hours premature when compared with observations. In addition to this, both the overall magnitudes of wet-hour frequency and the amplitude of its diurnal cycle are considerably higher than found in observations. As with the all-hour mean, for the wet-hour mean and frequency the choice of GCM or use of reanalysis does not change the timing of the diurnal minimum or maximum in a given RCM (CCLM4-8-17, RCA4, ALADIN63, HadREM-GA7-05). Considering wet-hour mean and frequency together indicates that the positive aspect of the EC-11 all-hour mean DCP (figures 2(a)–(b)), i.e. realistic amplitude, results from a cancellation of errors: a too-frequent convective triggering and too-light precipitation combine to produce a realistic amplitude for the all-hour mean DCP. At convection-permitting resolution, the CPM provides a

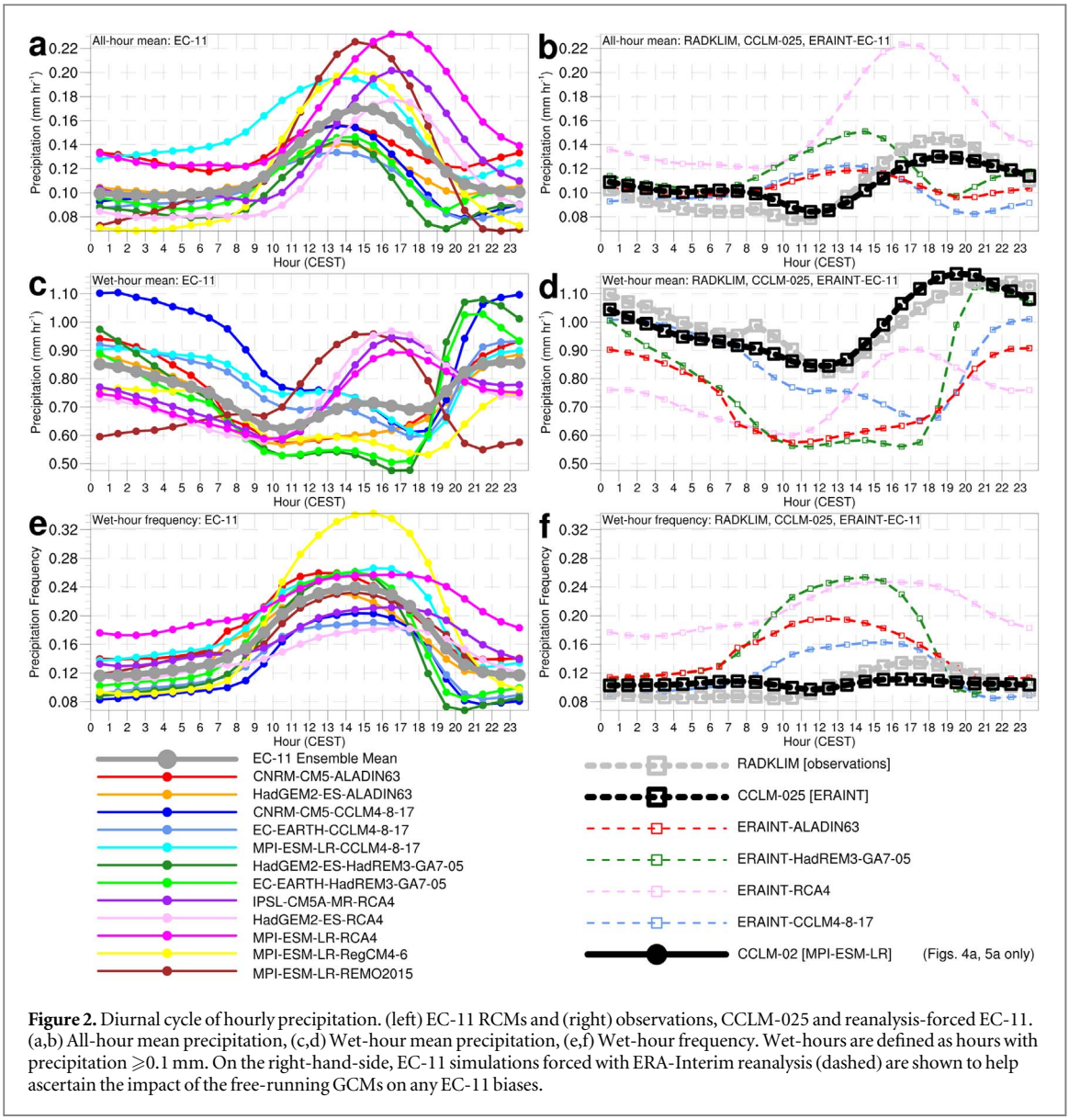

Figure 2. Diurnal cycle of hourly precipitation. (left) EC-11 RCMs and (right) observations, CCLM-025 and reanalysis-forced EC-11. (a,b) All-hour mean precipitation, (c,d) Wet-hour mean precipitation, (e,f) Wet-hour frequency. Wet-hours are defined as hours with precipitation $\geqslant$0.1 mm. On the right-hand-side, EC-11 simulations forced with ERA-Interim reanalysis (dashed) are shown to help ascertain the impact of the free-running GCMs on any EC-11 biases.

dramatic improvement on both its parent CCLM-11 and the EC-11 ensemble mean: CCLM-025 adds value by producing diurnal cycles of wet-hour mean and frequency which closely match both the magnitude and timing found in observations.

To assess how modelled biases change at even higher event intensities, we finish our evaluation by focusing on intense to extreme events (figure 3), namely the relative probability that an intense or extreme precipitation quantile will be exceeded at a given hour of the day. In both observations and CCLM-025, the relative probability that the 0.999-quantile—roughly equivalent to the two strongest events each summer—will be exceeded peaks at 2000 CEST, with a minimum at 1200 CEST. The peak exceedance probability is four times higher than the minimum and the highest exceedance probabilities are all found from 1700 CEST to midnight. In the EC-11 ensemble, however, the timing of 0.999-quantile exceedances is poorly represented, with some of the lowest exceedance probabilities found in the late-afternoon and early evening; exceedance probabilities at these times are near-maximum in observations and CCLM-025. The EC-11 ensemble instead shows peak exceedance probabilities from roughly 2200 to 0200 CEST. Additionally, and with the exception of REMO2015, no 0.11° RCM has a diurnal amplitude as high as that found in observations or CCLM-025. Moving to more extreme events, the observed relative probability of exceedance of the 0.9999-quantile—roughly equivalent to the four strongest events across the entire 18-summer analysis period—shows a similar diurnal curve to the 0.999-quantile, though with much higher amplitude. This is again well recreated by CCLM-025, e.g. same amplitude, though with detectable underestimation in the afternoon period. For the 0.11° RCMs, the timing errors of the exceedance maxima are similar to those found for the 0.999-quantile and the amplitude of the diurnal cycle is considerably lower than in observations or CCLM-025, with the exception of HadREM-GA7-05.

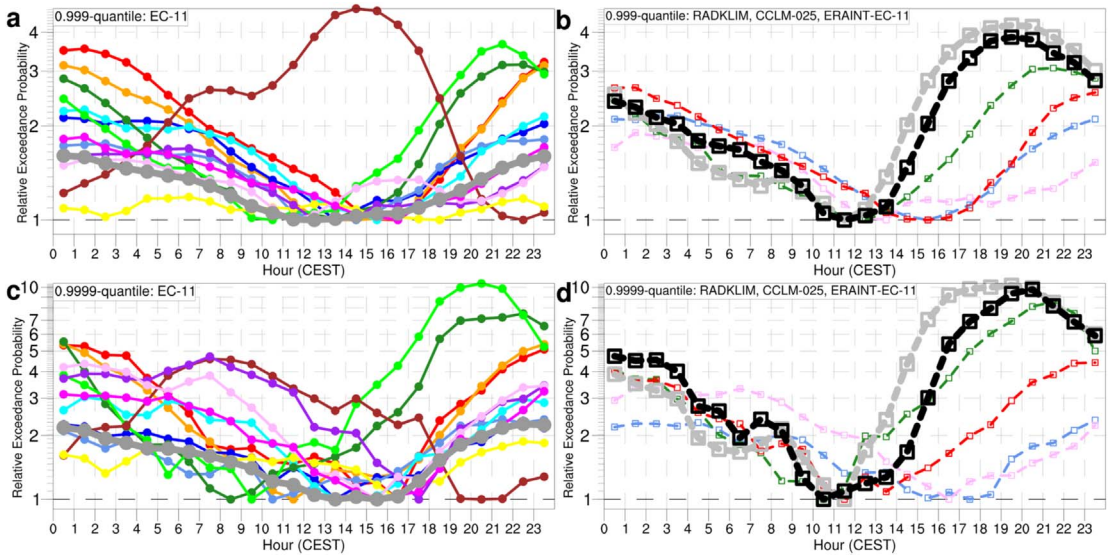

Figure 3. Hourly relative probabilities of exceedance of intense to extreme precipitation quantiles. (left) EC-11 RCMs and (right) observations, CCLM-025 and CCLM-11. (a,b) 0.999-quantile, (c,d) 0.9999-quantile. Relative probabilities are with respect to the hour of lowest probability, which is given a relative probability of 1. The ensemble mean is computed by averaging the exceedance probabilities across all RCMs and then computing a relative exceedance probability from this, rather than by taking the ensemble mean of the relative exceedance probabilities. Quantiles are based on all hours, i.e. without hour-of-day partitioning. On the right-hand-side, EC-11 simulations forced with ERA-Interim reanalysis (dashed) are shown to help ascertain the impact of biases in the free-running GCMs on any EC-11 biases. Note logarithmic *y*-axis. Colours are as in figure 2 legend.

EC-11 models thus produce intense to extreme events which are more evenly distributed across the day than in observations and CPMs, and also misrepresent the timing of the diurnal probability maximum for such events. Of the individual EC-11 ensemble members, HadREM3-GA7-05 best matches the observed diurnal cycle of exceedance probabilities (the diurnal maximum occurs too late, however, as reported in [81]. For the correct timing of intense to extreme events, it can be concluded that the CPM offers clear added value over the 0.11° RCMs, regardless of whether the 0.11° RCMs are forced by free-running GCMs or reanalysis. In EC-11 models, the timing biases for the probability of intense to extreme events differ considerably from the timing biases for the all-hour mean DCP. While the all-hour mean DCP peaks 3–4 hours prematurely in EC-11 models, the probability maximum for intense events has a diurnal peak delayed by 4–5 hours. These biases are likely related. A potential explanation is that excessive early-afternoon triggering of precipitation in EC-11 models prematurely removes CAPE and increases convective inhibition (CIN) so that there is a reduction in late-afternoon intense convection.

3.2. Future scaling of extremes and changes in mean precipitation at the diurnal scale

The overall more realistic representation of different aspects of the diurnal precipitation cycle in the CPM compared to the 0.11° RCMs (figures 2–3) indicates that we can have more confidence in projections of future changes to diurnal precipitation characteristics derived from CPMs. We thus firstly compare the future (2070-2099, RCP8.5) diurnal projections over the MUR19 analysis region between CCLM-02 and the EC-11 ensemble, and subsequently use any differences to aid interpretation of EC-11 diurnal projections across the eight PRUDENCE regions; the historical reference period is 1970-1999. In particular, using a CPM, MUR19 identified the possibility for strong diurnal differences in the future scaling (%/K) of intense to extreme hourly precipitation. In the MUR19 analysis region, maximum scaling was found in the morning and minimum scaling in the late afternoon. In this section we investigate whether EC-11 models also exhibit a diurnal signal for future precipitation changes and, if so, how this differs from that found in a CPM. We further investigate whether systematic differences in this diurnal signal exist between EC-11 models and PRUDENCE regions. Germany, the focus of the model evaluation in section 3.1, comprises the majority of the PRUDENCE region 'Mid Europe' (ME).

In the MUR19 analysis region (figure 4(a)), CCLM-02 shows a clear diurnal signal for the scaling of extreme hourly precipitation, with a morning peak scaling exceeding the CC rate and an afternoon sub-CC minimum. Many EC-11 GCM-RCM combinations also exhibit super-CC scaling and almost all combinations show a diurnal signal in the MUR19 analysis region, though there is considerable variance in amplitudes between individual EC-11 members (e.g. CNM-CR5-ALADIN63 versus MPI-ESM-LR-REMO2015). The amplitude of the diurnal signal in CCLM-02 is noticeably higher than in both its parent CCLM-11 and all other EC-11

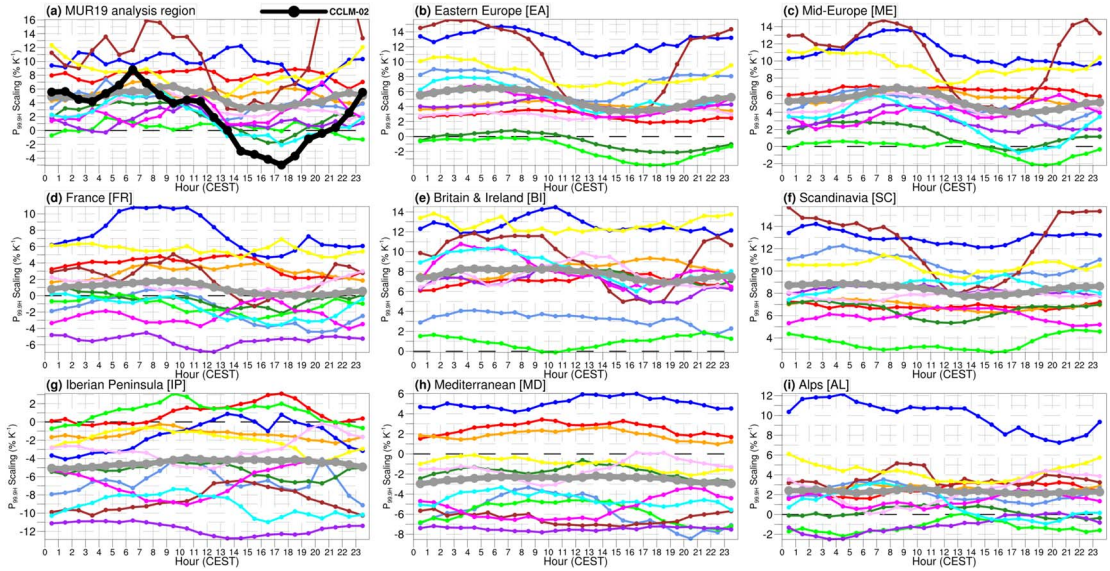

Figure 4. Diurnal scaling signal of extremes. Scaling (%/K) of 0.999-quantile 1-hour precipitation in the (a) MUR19 analysis region and (b–i) 8 PRUDENCE regions. Note that the 0.999-quantile is computed separately for each hour-of-day using all hours (i.e. wet and dry). For the MUR19 analysis region, the CCLM-02 CPM is represented by a thick black curve. EC-11 ensemble means are shown in thick grey. See figure 1 for regions and figure 2 for full legend.

models. Coupled with the CPM's more realistic representation of the diurnal distribution of intense to extreme events for the evaluation period, this suggests that EC-11 RCMs underestimate the amplitude of diurnal differences in the future scaling of intense precipitation. Interestingly, despite strong disagreement between the CPM and 0.11° RCMs on the relative hourly probabilities of 1-hour intense to extreme events in the evaluation period (figure 3), CCLM-02 and its parent CCLM-11 show close agreement for the future period on the timings of minimum and maximum scalings of 0.999-quantile diurnal hourly precipitation: the minimum hour matches exactly, while the maximum is just marginally displaced. This good agreement with the CPM extends to the EC-11 ensemble mean, providing grounds for optimism that the deficiencies of the EC-11 RCMs in recreating the characteristics of the evaluation period DCP do not fully preclude their utility for estimating future changes to the diurnal characteristics of intense precipitation. This further suggests that diurnal differences in future extreme scaling may be dominated by the large-scale environment rather than by small-scale processes which are only resolvable by CPMs.

Across the eight PRUDENCE regions (figures 4(b)–(i)), the EC-11 ensemble mean shows considerable regional variability in the diurnal signal of extreme precipitation scaling (%/K). This ranges from ensemble mean amplitudes of 3.5%/K in Mid and Eastern Europe, to close to 0%/K in the Alps and Mediterranean. Each EC-11 regional ensemble mean is furthermore accompanied by notable intra-ensemble variability in both the amplitude and magnitude of the future scalings, ranging from negative to super-CC scaling and with some RCMs showing a pronounced and others little-to-no diurnal signal. This suggests that a diurnal signal in intense precipitation scaling under climate change is (i) model dependent—at least in RCMs with parametrized convection—and (ii) regionally dependent, as postulated in MUR19. The model-dependency of the diurnal signal may, however, diminish or even disappear at convection-permitting resolution: recent studies suggest that precipitation projections in different RCMs and perturbed-physics ensembles converge at convection-permitting resolution [82, 83].

For future changes (%) to the diurnal cycle of all-hour mean precipitation, both the EC-11 ensemble mean and CCLM-02 again show clear diurnal signals for the MUR19 analysis region (figure 5(a)). The signal amplitude is again far greater in the CPM than in its parent CCLM-11 and most EC-11 models. The timing of the minimum and maximum changes is, however, in perfect agreement between CCLM-02 and both CCLM-11 and the EC-11 ensemble mean, adding confidence that EC-11 RCMs can accurately predict the times-of-day when diurnal differences in future changes are highest/lowest. Across the eight PRUDENCE regions (figures 5(b)–(i)), there is again strong regional variability in the amplitudes of the diurnal change signal; the regional ranking for the EC-11 ensemble mean diurnal amplitudes of mean precipitation change is in good agreement with the regional ranking for the scaling of intense events, suggesting that the former may be a good predictor for the latter, which is further investigated in section 3.3. Future changes in the diurnal cycles of mean wet-hour precipitation and wet-hour frequency are temporally similar to those for the all-hour mean, with the diurnal cycle of frequency changes exhibiting a higher amplitude than that of wet-hour mean changes (figures S2-3).

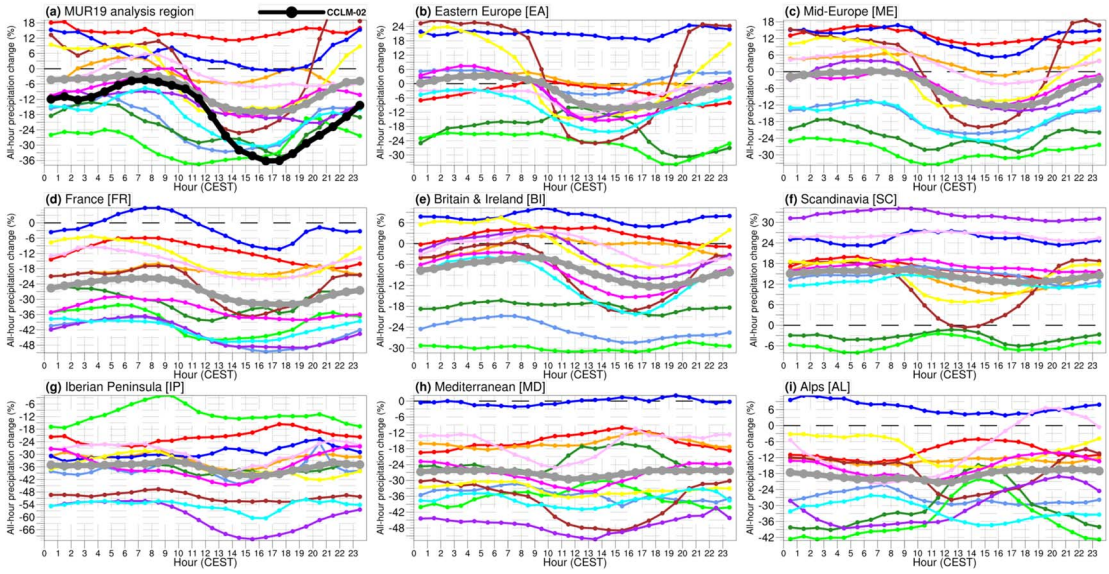

Figure 5. Diurnal signal of mean precipitation change. Diurnal mean future changes (%) of 1-hour precipitation in the (a) MUR19 analysis region and (b–i) 8 PRUDENCE regions. Note that the mean is computed separately for each hour-of-day using all hours (i.e. wet and dry). For the MUR19 analysis region, the CCLM-02 CPM is represented by a thick black curve. EC-11 ensemble means are shown in thick grey. See figure 1 for regions and figure 2 for full legend.

3.3. Relationship of the diurnal scaling signal to temperature and other changes

MUR19 performed a detailed analysis of the dynamical and thermodynamical environments underlying diurnal differences in the scaling of extreme precipitation events under climate change and proposed that regions in which mean warming considerably outstrips the increase in temperature at which late-afternoon extremes occur would have the potential for a diurnal future scaling signal similar to that found with CCLM-02 in the MUR19 analysis region (figure 4(a)), i.e. stronger scaling in the morning and weaker in the afternoon. The similarity of the timing of scaling minima/maxima between the EC-11 ensemble mean and the CPM in the MUR19 analysis region suggests that the mechanisms of change identified in the CPM by MUR19 may also be relevant within the EC-11 ensemble projections and across the different PRUDENCE regions. In this section we thus investigate whether the differences in the diurnal scaling signal (figure 4) between EC-11 models and PRUDENCE regions can be related to diurnal differences in the future changes of other meteorological parameters. To this end, we make use of available subdaily EC-11 variables to test if the mechanisms identified in MUR19 are also relevant in EC-11 models across the PRUDENCE regions. We further attempt to identify additional meteorological parameters from EC-11 RCMs whose diurnal changes may be related to the amplitude of the diurnal extreme scaling signal for a given region or RCM (see Methods for details).

The temperature at which precipitation extremes occur (T_E), and how this increases under climate change in comparison to the mean warming (ΔT_M), is known to be an important factor in the scaling magnitude of extremes [84–86]. We find that EC-11 RCMs and PRUDENCE regions which exhibit strong diurnal differences in T_E increase also tend to have the highest amplitude diurnal scaling signals (figure 6(a)), as proposed in MUR19. The linear regression model indicates that regions and RCMs in which ΔT_E in the AM (PM) period exceeds that in the PM (AM) period will tend to have stronger scaling in the former (latter), i.e. a positive (negative) amplitude for the diurnal scaling curve. An interesting aspect of the regression is that regions with high scaling signal amplitudes (MUR19, ME, EA and FR) occupy a similar latitude band, while regions with low scaling signal amplitudes (IP, MD, AL) are all further south. In the present climate, there is also a north-south gradient in JJA CIN over Europe, with the highest values in the south [87, 88]. The CIN gradient is expected to strengthen under climate change [89, 90]. This suggests that in regions where the amplitude of the diurnal scaling signal is high, the warmer and moister future climate brings morning conditions closer to the convective temperature, so that in these regions intense morning precipitation events more often occur at relatively higher temperatures. In regions where the amplitude of the diurnal scaling signal is low, on the other hand, the higher CIN limits the likelihood that the warmer and moister future morning conditions will approach the convective temperature, making T_E in these regions less skewed towards the higher morning temperatures and fewer morning events resulting from the convective temperature being reached.

As suggested by figures 4–5, diurnal differences in mean precipitation changes are also indicative of the diurnal scaling cycle's amplitude (figure 6(b)): regions and RCMs with large diurnal differences in mean precipitation changes also show large diurnal differences in the scaling of extreme precipitation. This is of

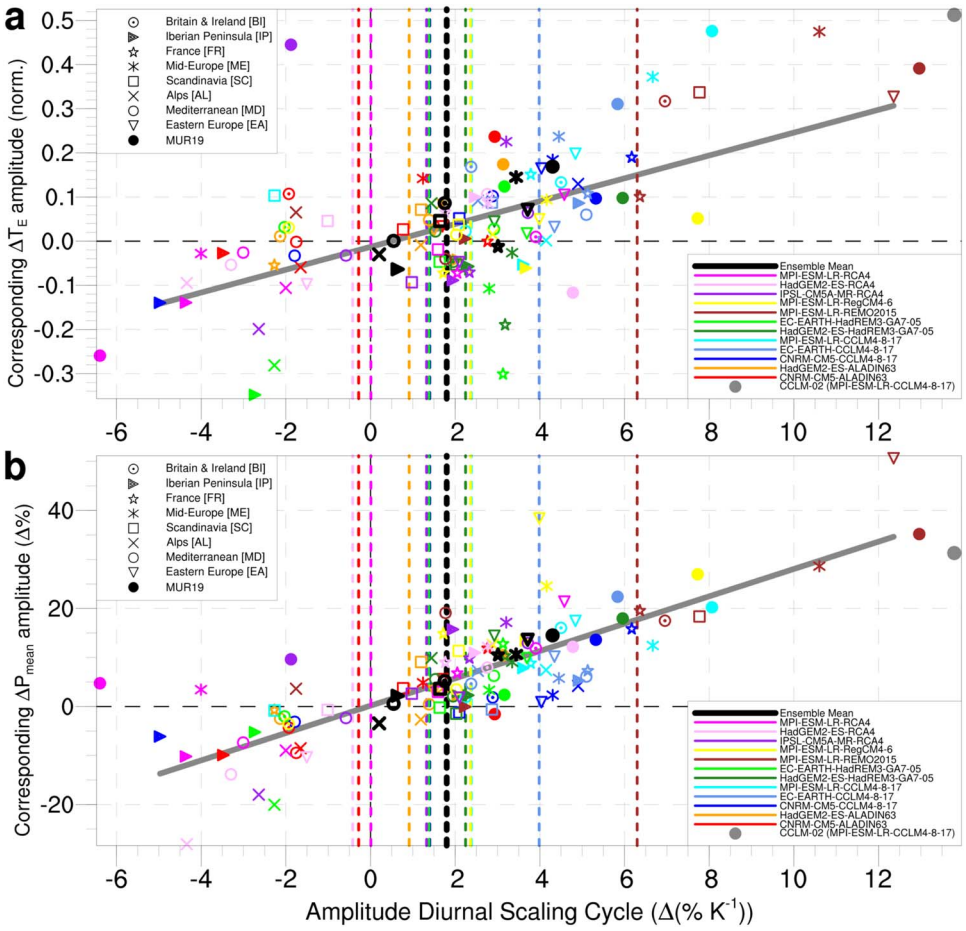

Figure 6. Relationship between amplitude of diurnal scaling cycle and other future changes. Amplitude (peak-to-trough) of the diurnal scaling curves (see figure 4) plotted against the corresponding diurnal differences in future changes of (a) T_E—the temperature at which 0.999-quantile 1-hour events occur—and (b) mean precipitation. A positive (negative) scaling amplitude corresponds to a scaling maximum (minimum) in the AM (PM) period. The diurnal differences in (a) and (b) are determined for the hours-of-day which correspond to the minimum and maximum scaling hours-of-day shown in figure 4. Diurnal differences in T_E changes are additionally normalized by the mean warming signal of the RCM. The regression lines are based on an area-weighted regression for the PRUDENCE regions only, i.e. the MUR19 region is excluded in order to avoid unnecessary duplication of grid-cells. The inter-regional scaling amplitude means for each RCM (vertical dashed lines) are likewise area weighted and exclude MUR19. See Methods for further details. Note that due to missing temperature data, the results in (a) for HadGEM2-ES-ALADIN63 are based on 20-year climatologies. Note the legend: black for ensemble/regional means, grey for CCLM-02 in MUR19 (top right).

potential utility, as the agreement between CCLM-02 and the EC-11 ensemble mean on the diurnal timings of minimum/maximum future changes in mean precipitation over the MUR19 analysis region (figure 5(a)) suggests that non-CPMs can also be used to predict the times of day at which future scaling of extremes will be highest or lowest. The associations between the variables in each linear regression show high statistical significance ($p < 1.e-8$). Aside from these thermodynamic variables, we did not find any evidence that regional differences in the diurnal scaling amplitude could be accounted for by future changes in the frequency of the large-scale circulation patterns which accompany precipitation extremes. Likewise, regional differences in vertical warming profiles also showed no statistically significant relationship (supplementary figures S4-5 and accompanying discussion).

The scatter plots (figure 6) further highlight the extent to which the amplitude of the diurnal scaling cycle in the CPM exceeds that found in the EC-11 RCMs: across all 108 diurnal series (9 regions, 12 GCM-RCM combinations), nowhere in the EC-11 ensemble is the amplitude of the diurnal scaling cycle as high as in the single CPM diurnal series (grey filled circle). The scatter plots further reveal that the RCM is an important factor in the diurnal scaling amplitude: averaging across all PRUDENCE regions, the different GCM-RCM means for combinations involving each of CCLM4-8-17, RCA4, HadREM-GA7-05 and ALADIN63 (other RCMs are only represented once) tend to be near to the means of other combinations involving the same RCM. The choice of GCM, meanwhile, shows no consistent relation to the amplitude of the diurnal scaling cycle. Using a different realization of the same GCM-RCM combination (MPI-ESM-LR-CCLM4-8-17) was found to produce some regional differences though not affect the overall conclusions (figures S6-7). At convection-permitting

resolution, the choice of RCM is likely less important as recent studies suggest that RCM precipitation climatologies and projections may converge at convection-permitting resolution [82, 83].

4. Further discussion and conclusions

Our study is to-date the first and largest multi-model analysis of the DCP and hourly precipitation, respectively, in the EC-11 ensemble. We have demonstrated the superior representation of the DCP in a CPM compared to the EC-11 ensemble, particularly with respect to the diurnal distribution of intense to extreme precipitation (figures 2 and 3). We have furthermore found a diurnal signal in future (RCP8.5 scenario) mean precipitation change and the scaling of intense to extreme events across multiple European regions, in both the EC-11 ensemble and in a CPM (figures 4 and 5). Here, we found a strongly amplified signal in the CPM compared to the EC-11 models and a reasonable temporal agreement between the diurnal signals of the CPM and EC-11 ensemble mean. We finally identified meteorological parameters (mean precipitation, temperature at which extremes occur) in the EC-11 RCMs for which diurnal differences in their future changes may be related to the amplitude of the diurnal signal of extreme precipitation scaling (figure 6), just as in the CPM.

For the evaluation period (2001–2018), the state-of-the-art EC-11 ensemble still retains the core deficiency in recreating the observed DCP found in lower-resolution models [13, 15, 21–26]: premature convective triggering gives an all-hour mean DCP that peaks too early in the afternoon (figure 2). The realistic amplitude we find for the ensemble mean EC-11 all-hour DCP turns out to be an error-cancellation based on excessive triggering of insufficiently intense events during the early afternoon. For the modelling of precipitation extremes, higher-resolution RCMs—even non-CPMs—have previously been shown to add value [30, 31, 36, 37]. With respect to the diurnal cycle, however, we show that the observed diurnal distribution of intense to extreme precipitation is completely misrepresented in EC-11 RCMs (figure 3). While observations and the CPM show probabilities for the exceedance of high-quantile thresholds which are heavily skewed towards the late-afternoon and evening in our evaluation region, EC-11 RCMs produce intense to extreme events which are distributed much more evenly across the day. Some of the lowest hourly threshold exceedance probabilities for intense to extreme hourly precipitation in EC-11 RCMs occur during hours when exceedance probabilities are near-maximum in observations (and the CPM), i.e. late afternoon. EC-11 models furthermore erroneously produce their corresponding threshold exceedance probability maximum during the night. This problem worsens as precipitation quantiles become more intense. At convection-permitting resolution, CCLM-025 not only greatly improves the representation of the diurnal cycles of all-hour precipitation [24, 42, 44, 91], wet-hour precipitation [92] and wet-hour frequency [92, 93], but also produces a realistic diurnal distribution of intense to extreme precipitation, despite this being absent in its parent EC-11 RCM (figures 2- 3). The relatively high resolution of the EC-11 models seems to add little value for the representation of the DCP, which clearly requires CPMs to be realistically captured, in particular for intense events. This supports the notion that the shortcomings of the simulated DCP in climate models are primarily a problem of convection parametrization schemes, more so than the role of model resolution [23, 27]. Indeed, even higher resolution RCMs (0.0625°) using convection parametrization schemes have displayed similar biases in the mean DCP [24] as those found here in EC-11 RCMs.

Looking to future changes in precipitation across the diurnal cycle, we have shown that the strong diurnal signal for the scaling (%/K) of intense to extreme hourly precipitation identified in MUR19 is neither unique to the MUR19 analysis region nor to CPMs (figure 4). A strong diurnal signal for the future scaling of intense to extreme hourly precipitation can also be found within the EC-11 ensemble, albeit often with considerable ensemble spread. The amplitude of the diurnal signal is highly variable between regions and RCMs, ranging from no clear diurnal signal (e.g. Mediterranean, Alps) to a prominent diurnal signal (e.g. Mid and Eastern Europe). This is not only the case for the scaling of intense 1-hour events, but also for future changes in diurnal mean hourly precipitation (figure 5). The ensemble spread of the EC-11 results presented here characterizes the overall range of projection uncertainty based on the current RCM and GCM state-of-the-art, for the chosen RCP8.5 scenario. Scenario uncertainty is not accounted for, nor are uncertainties related to systematic deficiencies in global and regional climate models in general, for example imperfect parametrization schemes or potential biases in synoptic-scale circulation. For the CPM, we cannot characterize its associated uncertainties due to the lack of a CPM ensemble and must instead be guided by its performance in the present climate. While there is evidence that precipitation projections from different RCMs converge at convection-permitting resolution [82, 83], CPM convergence is not guaranteed [94].

Comparing diurnal differences in future precipitation changes between a CPM over the MUR19 analysis region and the EC-11 RCMs reveals some key insights. Firstly, non-CPMs project much smaller diurnal differences in the scaling of intense to extreme precipitation. Across all 12 EC-11 GCM-RCM combinations in all 9 regions analysed, nowhere is the amplitude of the diurnal scaling signal so strong as that found in the single

CPM realization. With few exceptions, this also holds for changes in mean diurnal precipitation. Coupled with the more realistic DCP produced by the CPM for the present climate, this suggests that non-CPMs underestimate the magnitude of diurnal differences in future precipitation changes under climate change, particularly for intense to extreme rainfall. Secondly, despite clear differences in their representation of the present-climate DCP, the CPM shows good agreement with both its parent 0.11° RCM and the EC-11 ensemble mean on the hour-of-day of minimum and maximum future changes in the DCP, i.e. mean precipitation and scaling of intense to extreme events (at least for the particular region studied in MUR19, over central Europe). This adds credibility to the EC-11 projections and suggests that the large-scale environment is the dominant factor behind the existence of diurnal differences in future precipitation changes, rather than convective-scale processes which cannot be resolved in non-CPMs. Once the necessary large-scale changes are present and the convective temperature can be reached more often in the morning, then explicit simulation of deep convective processes in the CPM acts to amplify the diurnal scaling signal. Whether the agreement on the diurnal timing of minimum and maximum future changes would also be found with a continental-scale CPM [93, 95–97] which could potentially show much greater deviation from its parent model merits further investigation. There is furthermore no clear evidence that EC-11 models which perform better in the evaluation period also have closer agreement with the CPM future projections. Thirdly, meteorological parameters found to be relevant for a strong diurnal signal of extreme precipitation scaling in the CPM over the MUR19 analysis region (e.g. diurnal differences in changes in the temperature at which intense events occur and changes in mean precipitation) are also relevant in regions and RCMs in the EC-11 ensemble which exhibit a strong diurnal signal in their scaling of intense to extreme precipitation under climate change (figure 6). Together, these insights suggest that EC-11 RCMs offer utility for predicting the diurnal aspects of extreme precipitation scaling and mean changes in different regions, albeit with a probable underestimation of the amplitude of any detected diurnal signal.

To conclude, our results illustrate that a strong diurnal signal for future extreme [4] and mean precipitation change is a distinct feature in the EC-11 ensemble and also found in a CPM, which extends across different—though, importantly, not all—regions. The amplification of this diurnal climate change signal in the CPM with respect to that found in EC-11 RCMs adds further evidence that CPMs can substantially modulate the climate change signal of their parametrized-convection parent models [54, 55]. The state-of-the-art EC-11 ensemble is still, however, a useful tool for assessing diurnal variability in future precipitation changes. Our results point towards the potential benefit of continental-scale climate simulations with CPMs [93, 95–97]: the amplified diurnal change signal explicitly simulated by the CPM could have local- or even synoptic-scale feedbacks on the atmosphere. These feedbacks may, in turn, influence the aggregate statistics of other variables such as humidity, temperature and wind [98], and potentially their climate-change signals too. Such CPM simulations furthermore enable a more detailed process-based understanding of diurnal differences in future precipitation change [4] than is possible with models reliant on parametrization of convection. Our study thus finds some value in the EC-11 ensemble for studying future changes in precipitation at the diurnal scale, while also supporting the use of CPMs and moves towards coordinated climate simulations at convection-permitting resolution [98].

Acknowledgments

This study was funded by the German Ministry for Education and Science (Bundesmininsterium für Bildung und Forschung) through the ClimXtreme project, grant number 01LP1902H. The CCLM-02 simulations were performed as part of the EU H2020 project BINGO (www.projectbingo.eu), grant agreement 641739. The CCLM-11 simulations with ERA-Interim boundary forcing were also performed as part of the BINGO project, with EM further receiving partial support from the EUREX project of the Helmholtz Association (HRJRG-308). This work used resources of the Deutsches Klimarechenzentrum (DKRZ) granted by its Scientific Steering Committee (WLA) under project IDs bb0961 and bb1152. Supercomputing facilities were also provided by ZEDAT of the Freie Universität Berlin (https://doi.org/10.17169/refubium-26754), the North-German Supercomputing Alliance (HLRN, www.hlrn.de), and the Jülich Supercomputing Centre via the JARA computing time project JJSC39 and the John von Neumann Institute for Computing (NIC) project HKA19. Analyses were performed with the NCAR Command Language [99], R [100], CDO (https://code.mpimet.mpg.de/projects/cdo) and NCO (http://nco.sourceforge.net/). The authors thank Grigoriy Nikulin (SMHI) and all of the individual modelling groups who made their simulation data publicly available, as well as the German Weather Service for producing the RADKLIM dataset [76]. The authors further thank the CLM-Community (www.clm-community.eu) for developing and maintaining the CCLM model.

Data availability statement

Almost all 0.11° EURO-CORDEX data used in this analysis are available via the ESGF data nodes. For example, https://esgf-data.dkrz.de/search/cordex-dkrz/. The only exception is the hourly precipitation data for CCLM4-8-17 which, at the time of writing, are not yet available via the ESGF nodes; these must be requested directly from the CLM-Community (https://www.clm-community.eu/). The CCLM-11 simulations with ERA-Interim boundary forcing performed by the present authors [73] have been archived under an open access license at the DKRZ Long Term Archive (https://cera-www.dkrz.de/WDCC/ui/cerasearch/entry?acronym=DKRZ_LTA_961_ds00002). The CCLM-02 simulations used in this study and MUR19 have also been archived under an open access license at the DKRZ Long Term Archive (https://cera-www.dkrz.de/WDCC/ui/cerasearch/entry?acronym=DKRZ_LTA_961_ds00006) and are citable as [101]. The CCLM-025 simulations have similarly been archived at the DKRZ Long Term Archive (https://cera-www.dkrz.de/WDCC/ui/cerasearch/entry?acronym=DKRZ_LTA_961_ds00009). The RADKLIM dataset [76] of hourly precipitation is available from the German Weather Service (DWD) at https://doi.org/10.5676/DWD/RADKLIM_RW_V2017.002.

References

[1] Abdou K, Parker D J, Brooks B, Kalthoff N and Lebel T 2010 The diurnal cycle of lower boundary-layer wind in the West African monsoon *Q. J. R. Meteorolog. Soc.* **136** 66–76
[2] Barthelmie R, Grisogono B and Pryor S 1996 Observations and simulations of diurnal cycles of near-surface wind speeds over land and sea *Journal of Geophysical Research: Atmospheres* **101** 21327–37
[3] Hentgen L, Ban N, Kröner N, Leutwyler D and Schär C 2019 Clouds in Convection-Resolving Climate Simulations Over Europe *Journal of Geophysical Research: Atmospheres* **124** 3849–70
[4] Meredith E P, Ulbrich U and Rust H W 2019 The diurnal nature of future extreme precipitation intensification *Geophys. Res. Lett.* **46** 7680–9
[5] Nesbitt S W, Gochis D J and Lang T J 2008 The diurnal cycle of clouds and precipitation along the Sierra Madre Occidental observed during NAME-2004: Implications for warm season precipitation estimation in complex terrain *Journal of Hydrometeorology* **9** 728–43
[6] Pfeifroth U, Hollmann R and Ahrens B 2012 Cloud cover diurnal cycles in satellite data and regional climate model simulations *Meteorol. Z.* **21** 551–60
[7] Werner P C and Gerstengarbe F-W 2004 Changes of the diurnal cycle structures of selected meteorological parameters of Potsdam Station for the summer season *Climate Research* **26** 131–8
[8] Yang G-Y and Slingo J 2001 The diurnal cycle in the tropics *Mon. Weather Rev.* **129** 784–801
[9] Dai A 2001 Global precipitation and thunderstorm frequencies. Part II: Diurnal variations *J. Clim.* **14** 1112–28
[10] Dai A, Lin X and Hsu K-L 2007 The frequency, intensity, and diurnal cycle of precipitation in surface and satellite observations over low-and mid-latitudes *Clim. Dyn.* **29** 727–44
[11] Ghada W, Yuan Y, Wastl C, Estrella N and Menzel A 2019 Precipitation Diurnal Cycle in Germany Linked to Large-Scale Weather Circulations *Atmosphere* **10** 545
[12] Paulat M, Frei C, Hagen M and Wernli H 2008 A gridded dataset of hourly precipitation in Germany: Its construction, climatology and application *Meteorol. Z.* **17** 719–32
[13] Giles J A, Ruscica R C and Menéndez C G 2020 The diurnal cycle of precipitation over South America represented by five gridded datasets *Int. J. Climatol.* **40** 668–86
[14] Panziera L, Gabella M, Germann U and O Martius 2018 A 12-year radar-based climatology of daily and sub-daily extreme precipitation over the Swiss Alps *Int. J. Climatol.* **38** 3749–69
[15] Jeong J-H, Walther A, Nikulin G, Chen D and Jones C 2011 Diurnal cycle of precipitation amount and frequency in Sweden: observation versus model simulation *Tellus A: Dynamic Meteorology and Oceanography* **63** 664–74
[16] Hendon H H and Woodberry K 1993 The diurnal cycle of tropical convection *Journal of Geophysical Research: Atmospheres* **98** 16623–37
[17] Dai A, Giorgi F and Trenberth K E 1999 Observed and model-simulated diurnal cycles of precipitation over the contiguous United States *Journal of Geophysical Research: Atmospheres* **104** 6377–402
[18] Vernekar A D, Kirtman B P and Fennessy M J 2003 Low-level jets and their effects on the South American summer climate as simulated by the NCEP Eta Model *J. Clim.* **16** 297–311
[19] Hitchens N M, Brooks H E and Schumacher R S 2013 Spatial and temporal characteristics of heavy hourly rainfall in the United States *Mon. Weather Rev.* **141** 4564–75
[20] Zhang G, Cook K H and Vizy E K 2016 The diurnal cycle of warm season rainfall over West Africa. Part I: Observational analysis *J. Clim.* **29** 8423–37
[21] Brockhaus P, Lüthi D and Schär C 2008 Aspects of the diurnal cycle in a regional climate model *Meteorol. Z.* **17** 433–43
[22] Dai A and Trenberth K E 2004 The Diurnal Cycle and Its Depiction in the Community Climate System Model *J. Clim.* **17** 930–51
[23] Dirmeyer P A *et al* 2012 Simulating the diurnal cycle of rainfall in global climate models: Resolution versus parameterization *Clim. Dyn.* **39** 399–418
[24] Fosser G, Khodayar S and Berg P 2015 Benefit of convection permitting climate model simulations in the representation of convective precipitation *Clim. Dyn.* **44** 45–60
[25] Lin X, Randall D A and Fowler L D 2000 Diurnal variability of the hydrologic cycle and radiative fluxes: Comparisons between observations and a GCM *J. Clim.* **13** 4159–79
[26] Mooney P, Mulligan F and Broderick C 2016 Diurnal cycle of precipitation over the British Isles in a 0.44° WRF multiphysics regional climate ensemble over the period 1990–1995 *Clim. Dyn.* **47** 3281–300
[27] Vergara-Temprado J, Ban N, Panosetti D, Schlemmer L and Schär C 2020 Climate models permit convection at much coarser resolutions than previously considered. *J. Clim.* **33** 1915–33
[28] Kain J S 2004 The Kain-Fritsch convective parameterization: an update *J. Appl. Meteorol.* **43** 170–81

[29] Tiedtke M 1989 A comprehensive mass flux scheme for cumulus parameterization in large-scale models *Mon. Weather Rev.* **117** 1779–800
[30] Di Luca A, de Elía R and Laprise R 2012 Potential for added value in precipitation simulated by high-resolution nested regional climate models and observations *Clim. Dyn.* **38** 1229–47
[31] Feser F, Rockel B, von Storch H, Winterfeldt J and Zahn M 2011 Regional climate models add value to global model data: a review and selected examples *B. Am. Meteorol. Soc.* **92** 1181–92
[32] Giorgi F 2019 Thirty years of regional climate modeling: where are we and where are we going next? *Journal of Geophysical Research: Atmospheres* **124** 5696–723
[33] Rockel B 2015 The regional downscaling approach: a brief history and recent advances *Current Climate Change Reports* **1** 22–9
[34] Rummukainen M 2016 Added value in regional climate modeling *Wiley Interdiscip. Rev. Clim. Change* **7** 145–59
[35] Giorgi F *et al* 2009 Addressing climate information needs at the regional level: the CORDEX framework *World Meteorological Organization (WMO) Bulletin* **58** 175
[36] Heikkilä U, Sandvik A and Sorteberg A 2011 Dynamical downscaling of ERA-40 in complex terrain using the WRF regional climate model *Clim. Dyn.* **37** 1551–64
[37] Torma C, Giorgi F and Coppola E 2015 Added value of regional climate modeling over areas characterized by complex terrain - Precipitation over the Alps *J. Geophys. Res.-Atmos.* **120** 3957–72
[38] Becker N 2016 *Großskalige Sekundärzirkulationen im regionalen Klimamodell COSMO-CLM. PhD thesis* Freie Universität Berlin
[39] Becker N, Ulbrich U and Klein R 2015 Systematic large-scale secondary circulations in a regional climate model *Geophys. Res. Lett.* **42** 4142–9
[40] Becker N, Ulbrich U and Klein R 2018 Large-scale secondary circulations in a limited area model-the impact of lateral boundaries and resolution *Tellus A: Dynamic Meteorology and Oceanography* **70** 1–15
[41] Hohenegger C, Brockhaus P and Schär C 2008 Towards climate simulations at cloud-resolving scales *Meteorol. Z.* **17** 383–94
[42] Kendon E J, Roberts N M, Senior C A and Roberts M J 2012 Realism of rainfall in a very high-resolution regional climate model *J. Clim.* **25** 5791–806
[43] Armon M, Marra F, Enzel Y and Rostkier-Edelstein D 2020 Radar-based characterisation of heavy precipitation in the eastern Mediterranean and its representation in a convection-permitting model *Hydrology & Earth System Sciences* **24**
[44] Brisson E, Van Weverberg K, Demuzere M, Devis A, Saeed S, Stengel M and van Lipzig N P 2016 How well can a convection-permitting climate model reproduce decadal statistics of precipitation, temperature and cloud characteristics? *Clim. Dyn.* **47** 3043–61
[45] Knist S, Goergen K and Simmer C 2020 Evaluation and projected changes of precipitation statistics in convection-permitting WRF climate simulations over Central Europe *Clim. Dyn.* **55** 325–41
[46] Piazza M, Prein A F, Truhetz H and Csaki A 2019 On the sensitivity of precipitation in convection-permitting climate simulations in the Eastern Alpine region *Meteorol. Z.* **28** 323–46
[47] Zittis G, Bruggeman A, Camera C, Hadjinicolaou P and Lelieveld J 2017 The added value of convection permitting simulations of extreme precipitation events over the eastern Mediterranean *Atmos. Res.* **191** 20–33
[48] Prein A F, Gobiet A, Suklitsch M, Truhetz H, Awan N, Keuler K and Georgievski G 2013 Added value of convection permitting seasonal simulations *Clim. Dyn.* **41** 2655–77
[49] Prein A F *et al* 2015 A review on regional convection-permitting climate modeling: Demonstrations, prospects, and challenges *Rev. Geophys.* **53** 323–61
[50] Weisman M L, Davis C, Wang W, Manning K W and Klemp J B 2008 Experiences with 0-36-h explicit convective forecasts with the WRF-ARW model *Weather Forecasting* **23** 407–37
[51] Meredith E P, Ulbrich U and Rust H W 2020 Subhourly rainfall in a convection-permitting model *Environ. Res. Lett.* **15** 034031
[52] Purr C, Brisson E and Ahrens B 2019 Convective Shower Characteristics Simulated with the Convection-Permitting Climate Model COSMO-CLM *Atmosphere* **10** 810
[53] Brisson E, Brendel C, Herzog S and Ahrens B 2018 Lagrangian evaluation of convective shower characteristics in a convection-permitting model *Meteorol. Z.* **27** 59–66
[54] Kendon E J, Roberts N M, Fowler H J, Roberts M J, Chan S C and Senior C A 2014 Heavier summer downpours with climate change revealed by weather forecast resolution model *Nat. Clim. Change* **4** 570–6
[55] Meredith E P, Maraun D, Semenov V A and Park W 2015 Evidence for added value of convection-permitting models for studying changes in extreme precipitation *J. Geophys. Res.-Atmos* **120** 12500–13
[56] Allen M R and Ingram W J 2002 Constraints on future changes in climate and the hydrologic cycle *Nature* **419** 224
[57] Fischer E M and Knutti R 2016 Observed heavy precipitation increase confirms theory and early models *Nat. Clim. Change* **6** 986
[58] Trenberth K E 1999 Conceptual Framework for Changes of Extremes of the Hydrological Cycle with Climate Change *Clim. Change* **42** 327–39
[59] Davy R, Esau I, Chernokulsky A, Outten S and Zilitinkevich S 2017 Diurnal asymmetry to the observed global warming *Int. J. Climatol.* **37** 79–93
[60] Karl T R, Jones P D, Knight R W, Kukla G, Plummer N, Razuvayev V, Gallo K P, Lindseay J, Charlson R J and Peterson T C 1993 Asymmetric trends of daily maximum and minimum temperature *Papers in Natural Resources* **74** 185
[61] Lindvall J and Svensson G 2015 The diurnal temperature range in the CMIP5 models *Clim. Dyn.* **44** 405–21
[62] Jacob D *et al* 2014 EURO-CORDEX: new high-resolution climate change projections for European impact research *Reg. Environ. Change* **14** 563–78
[63] Jacob D *et al* 2020 Regional climate downscaling over Europe: perspectives from the EURO-CORDEX community *Regional Environmental Change* **20**
[64] Kotlarski S, Bosshard T, Lüthi D, Pall P and Schär C 2012 Elevation gradients of European climate change in the regional climate model COSMO-CLM *Clim. Change* **112** 189–215
[65] Prein A *et al* 2016 Precipitation in the EURO-CORDEX 0.11° and 0.44° simulations: high resolution, high benefits? *Clim. Dyn.* **46** 383–412
[66] Berg P, Christensen O B, Klehmet K, Lenderink G, Olsson J, Teichmann C and Yang W 2019 Summertime precipitation extremes in a EURO-CORDEX 0.11° ensemble at an hourly resolution *Natural Hazards and Earth System Sciences* **19** 957–71
[67] Déqué M, Rowell D, Lüthi D, Giorgi F, Christensen J, Rockel B, Jacob D, Kjellström E, De Castro M and van den Hurk B 2007 An intercomparison of regional climate simulations for Europe: assessing uncertainties in model projections *Clim. Change* **81** 53–70
[68] Paeth H *et al* 2011 Progress in regional downscaling of West African precipitation *Atmos. Sci. Lett.* **12** 75–82

[69] Mezghani A, Dobler A, Benestad R, Haugen J E, Parding K M, Piniewski M and Kundzewicz Z W 2019 Subsampling impact on the climate change signal over poland based on simulations from statistical and dynamical downscaling *Journal of Applied Meteorology and Climatology* **58** 1061–78
[70] Sørland S L, Schär C, Lüthi D and Kjellström E 2018 Bias patterns and climate change signals in GCM-RCM model chains *Environ. Res. Lett.* **13** 074017
[71] Dee D P *et al* 2011 The ERA-Interim reanalysis: configuration and performance of the data assimilation system. *Q. J. R. Meteor. Soc.* **137** 553–97
[72] Rockel B, Will A and Hense A 2008 The regional climate model COSMO-CLM (CCLM) *Meteorol. Z.* **17** 347–8
[73] Meredith E P and Ulbrich U 2018 *BINGO EURO-CORDEX Evaluation. World Data Center for Climate (WDCC) at DKRZ* (http://cera-www.dkrz.de/WDCC/ui/Compact.jsp?acronym=DKRZ_LTA_961_ds00002
[74] Meredith E P, Rust H W and Ulbrich U 2018 A classification algorithm for selective dynamical downscaling of precipitation extremes *Hydrol. Earth Syst. Sci.* **22** 4183–200
[75] Giorgetta M A *et al* 2013 Climate and carbon cycle changes from 1850 to 2100 in MPI-ESM simulations for the Coupled Model Intercomparison Project phase 5 *Journal of Advances in Modeling Earth Systems* **5** 572–97
[76] Winterrath T, Brendel C, Hafer M, Junghänel T, Klameth A, Lengfeld K, Walawender E, Weigl E and Becker A 2018 RADKLIM Version 2017.002: Reprocessed gauge-adjusted radar data, one-hour precipitation sums (RW) *Deutscher Wetterdienst (DWD)* doi:(10.5676/DWD/RADKLIM_RW_V2017.002
[77] Zhang X, Zwiers F W, Li G, Wan H and Cannon A J 2017 Complexity in estimating past and future extreme short-duration rainfall *Nat. Geosci.* **10** 255
[78] Christensen J H and Christensen O B 2007 A summary of the PRUDENCE model projections of changes in European climate by the end of this century *Clim. Change* **81** 7–30
[79] Burgueño A, Austin J, Vilar E and Puigcerver M 1987 Analysis of moderate and intense rainfall rates continuously recorded over half a century and influence on microwave communications planning and rain-rate data acquisition *IEEE Trans. Commun.* **35** 382–95
[80] Casas M C, Codina B, Redano A and Lorente J 2004 A methodology to classify extreme rainfall events in the western Mediterranean area *Theor. Appl. Climatol.* **77** 139–50
[81] Beranová R, Kysely J and Hanel M 2018 Characteristics of sub-daily precipitation extremes in observed data and regional climate model simulations *Theor. Appl. Climatol.* **132** 515–27
[82] Fosser G, Kendon E J, Stephenson D and Tucker S 2020 Convection-permitting models offer promise of more certain extreme rainfall projections *Geophys. Res. Lett.* **47** e2020GL088151
[83] Kendon E J, Ban N, Roberts N M, Fowler H J, Roberts M J, Chan S C, Evans J P, Fosser G and Wilkinson J M 2017 Do convection-permitting regional climate models improve projections of future precipitation change? *Bull. Am. Meteorol. Soc.* **98** 79–93
[84] O'Gorman P A and Schneider T 2009 Scaling of precipitation extremes over a wide range of climates simulated with an idealized GCM *J. Clim.* **22** 5676–85
[85] Pfahl S, O'Gorman P A and Fischer E M 2017 Understanding the regional pattern of projected future changes in extreme precipitation *Nat. Clim. Change* **7** 423
[86] Wang G, Wang D, Trenberth K E, Erfanian A, Yu M, Bosilovich M G and Parr D T 2017 The peak structure and future changes of the relationships between extreme precipitation and temperature *Nat. Clim. Change* **7** 268
[87] Riemann-Campe K, Fraedrich K and Lunkeit F 2009 Global climatology of convective available potential energy (CAPE) and convective inhibition (CIN) in ERA-40 reanalysis *Atmos. Res.* **93** 534–45
[88] Taszarek M, Brooks H E, Czernecki B, Szuster P and Fortuniak K 2018 Climatological aspects of convective parameters over Europe: a comparison of ERA-interim and sounding data *J. Clim.* **31** 4281–308
[89] Chen J, Dai A, Zhang Y and Rasmussen K L 2020 Changes in convective available potential energy and convective inhibition under global warming *J. Clim.* **33** 2025–50
[90] Sander J 2011 Extremwetterereignisse im Klimawandel: Bewertung der derzeitigen und zukünftigen Gefährdung *PhD thesis* Ludwig-Maximilians-Universität München (http://nbn-resolving.de/urn:nbn:de:bvb:19-128168
[91] Ban N, Schmidli J and Schär C 2014 Evaluation of the convection-resolving regional climate modeling approach in decade-long simulations *J. Geophys. Res.-Atmos.* **119** 7889–907
[92] Jin E K, Choi I-J, Kim S-Y and Han J-Y 2016 Impact of model resolution on the simulation of diurnal variations of precipitation over East Asia *Journal of Geophysical Research: Atmospheres* **121** 1652–70
[93] Leutwyler D, Lüthi D, Ban N, Fuhrer O and Schär C 2017 Evaluation of the convection-resolving climate modeling approach on continental scales *Journal of Geophysical Research: Atmospheres* **122** 5237–58
[94] Jucker M, Lane T P, Vincent C L, Webster S, Wales S A and Louf V 2020 Locally forced convection in subkilometre-scale simulations with the Unified Model and WRF *Q. J. R. Meteorolog. Soc.* **146** 3450–65
[95] Berthou S, Kendon E J, Chan S C, Ban N, Leutwyler D, Schär C and Fosser G 2018 Pan-European climate at convection-permitting scale: a model intercomparison study *Clim. Dyn.* **55** 35–59
[96] Chan S C, Kendon E J, Berthou S, Fosser G, Lewis E and Fowler H J 2020 Europe-wide precipitation projections at convection permitting scale with the unified model *Clim. Dyn.* **55** 409–28
[97] Liu C *et al* 2017 Continental-scale convection-permitting modeling of the current and future climate of North America *Clim. Dyn.* **49** 71–95
[98] Coppola E *et al* 2020 A first-of-its-kind multi-model convection permitting ensemble for investigating convective phenomena over europe and the mediterranean *Clim. Dyn.* **55** 3–34
[99] NCL 2018 The NCAR Command Language (Version 6.5.0) [Software] *Boulder, Colorado: UCAR/NCAR/CISL/TDD* (http://www.ncl.ucar.edu/ (https://doi.org/10.5065/D6WD3XH5)
[100] Core Team R 2018 *R: A Language and Environment for Statistical Computing. R Foundation for Statistical Computing, Vienna, Austria* (https://www.R-project.org/
[101] Meredith E P, Ulbrich U and Rust H W 2019b *BINGO Wupper 0.02 Degree Climate Simulations. World Data Center for Climate (WDCC) at DKRZ* (http://cera-www.dkrz.de/WDCC/ui/Compact.jsp?acronym=DKRZ_LTA_961_ds00006)
[102] Guérémy J 2011 A continuous buoyancy based convection scheme: one-and three-dimensional validation *Tellus A: Dynamic Meteorology and Oceanography* **63** 687–706
[103] Piriou J-M, Redelsperger J-L, Geleyn J-F, Lafore J-P and F Guichard 2007 An approach for convective parameterization with memory: Separating microphysics and transport in grid-scale equations *J. Atmos. Sci.* **64** 4127–39
[104] Gregory D and Rowntree P 1990 A mass flux convection scheme with representation of cloud ensemble characteristics and stability-dependent closure *Mon. Weather Rev.* **118** 1483–506

[105] Kain J S and Fritsch J M 1990 A one-dimensional entraining/detraining plume model and its application in convective parameterization *J. Atmos. Sci.* **47** 2784–802
[106] Kain J S and Fritsch J M 1993 Convective parameterization for mesoscale models: The Kain-Fritsch scheme *The representation of cumulus convection in numerical models* (Springer) 165–70
[107] Nordeng T 1994 Extended versions of the convection parametrization scheme at ECMWF and their impact upon the mean climate and transient activity of the model in the tropics *ECMWF Res. Dep. Tech. Memo.* 41